# FEM - ANALYSIS OF EDDY CURRENTS IN A BLDC STATOR LINER

Ovidiu CRAIU[1], Teodor-Ionuț ICHIM[2]

*The paper presents a numerical analysis of the eddy currents in a Brushless DC Motor (BLDC) with a special design. That is a capped motor with cylindrical liners on the stator and rotor used for stopping the hydraulic cooling fluid penetrating the motor.*

*A Computer-Aided-Design (CAD) of a BLDC was conducted using a Finite Element Method (FEM) electromagnetic field model for optimizing the shape of the electromagnetic torque versus rotor position. Then, the model was coupled with stator electric circuit equations and back electromotive force (EMF) was determined.*

*As the motor has high speed, eddy currents in the stator liner generate important losses and act as a brake to the rotor. To determine these losses with accuracy results from a 2D and a 3D FEM model were compared.*

**Keywords**: brushless DC Motor, eddy currents, torque ripple, Finite Element Method, electromotive force

## 1. Introduction

A common problem in designing high-speed BLDCs is dealing with centrifugal forces. One of the solutions to overcome the issue is to cover the rotor permanent magnets (PM) with a cylindrical liner (the so-called canned motors). Sometimes, to prevent hydraulic fluid or other particles to enter stator slots, the stator is also protected by a liner. In this latter case, the fast-moving magnets may induce high eddy currents in the stator liner. Together with higher frictional torque, the eddy currents are generating an important breaking torque, reducing motor efficiency. That is why, identifying materials with low electric conductivity [1] or making the stator liner of non-conductive materials such as nonmetallic, are solutions adopted by many. In addition to breaking torque, eddy current losses add to winding Joule losses making the motor cooling more challenging [2].

A second, equally important aspect in designing high-speed BLDC, is sizing the winding properly, so that enough voltage headroom remains at motor high speed, to allow generating the needed current. A too high number of coil

[1] Associate Professor at Electrical Engineering Faculty, Polytechnic Institute of Bucharest, email: ocraiu@yahoo.com

[2] Engineer at ICPE.SA and a PhD student at Electrical Engineering Faculty, University Polytechnic Institute of Bucharest, email: ichim_teodor@yahoo.com

turns may produce a motor back EMF too close to the supplied voltage, while a reduced number of turns will not use efficiently the available voltage and will require a higher current [3, 9].

In this paper, a study of a BLDC operating at a rotational speed of 12,500 rpm (corresponding to an angular velocity of 1,309 rad/s), as well as different computation manners of the eddy currents in the stator lining are presented. Using field-circuit FEM models, it was possible to compute the no-load voltage (motor back EMF), as well as the load phase and line-to-line voltages. To determine the right number of turns, the load terminal voltage magnitude must be as close as possible to the supply peak voltage. Apart from using all available voltage, opting for a higher number of turns would allow the motor to operate at a smaller current for obtaining the same torque while reducing Joule losses and enhancing motor efficiency [4].

## 2. FEM Torque optimization

The BLDC was designed using professional software COMSOL Multiphysics to generate a FEM model (fig.1) [5]. Consecutive, step-by-step, quasi-stationary magnetic field problems are computed, governed by the equation:

$$\nabla \times \left( \frac{1}{\mu} \nabla \times \mathbf{A} \right) = \mathbf{J} - \sigma \frac{\partial \mathbf{A}}{\partial t} + \nabla \times \left( \frac{1}{\mu} \mathbf{B}_r \right) \tag{1}$$

with **A** the magnetic vector potential, **J** the current density, and $\mathbf{J}_F = \sigma \cdot \partial \mathbf{A} / \partial \mathrm{t}$ eddy currents in the stator liner. Motor permanent magnets are modeled considering their linear demagnetization curve defined by remnant induction $\mathbf{B}_\mathrm{r}$ and equivalent magnetic permeability $\mu$ [6].

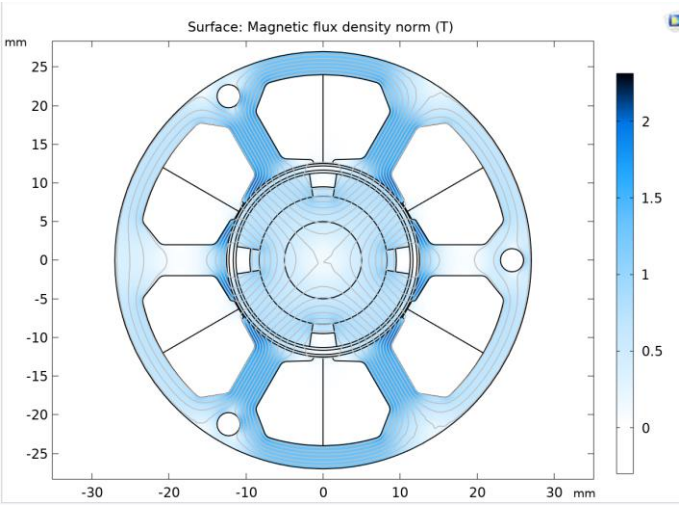


Fig. 1. FEM field model: magnetic flux density distribution and field lines.

The electromagnetic torque was computed for subsequent rotor positions considering the current constant in two of the three wye-connected motor phases, during the interval between two consecutive commutations. This interval represents 1/6th of the electric period, which, for the studied motor with p = 2 pole pairs, is T = $2.4 \times 10^{-3}$s (at an angular velocity of 1,309 rad/s). To achieve a good resolution of the torque-time curve, the time-interval of $4 \times 10^{-4}$s between commutations was divided into 40 time-steps of $1 \times 10^{-5}$s. The motor torque was computed for each such step using eq. (2). Rotor movement was simulated using COMSOL module "*Rotating Machinery, Magnetic*". This allows connecting the stator fixed discretization mesh with the rotor moving mesh through a slipping surface placed in the airgap, without rebuilding the geometry at each subsequent moving step [5,10].

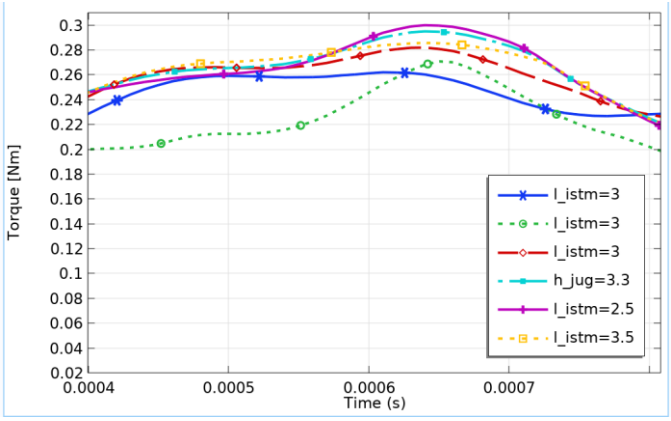


a) Torque-time variation curves for different slot openings *l_istm*.

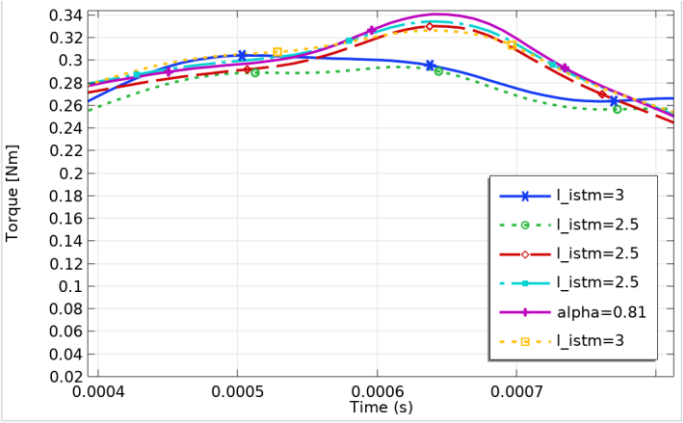


b) Torque-time variation curves for different slot openings *l_istm* and pole pitch *alpha*.

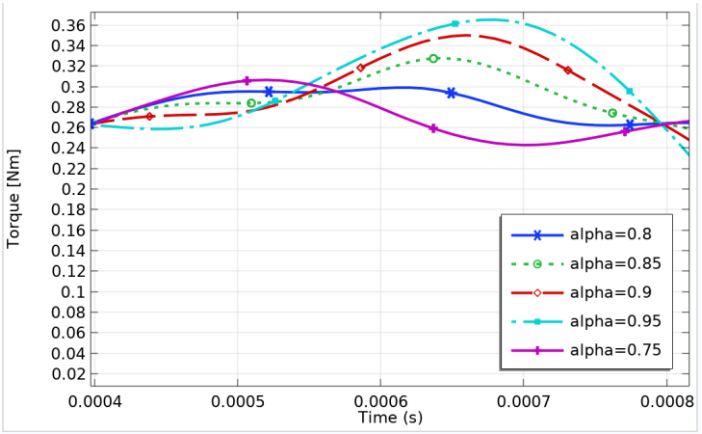


c) Torque-time variation curves for different pole pitch values *alpha*.

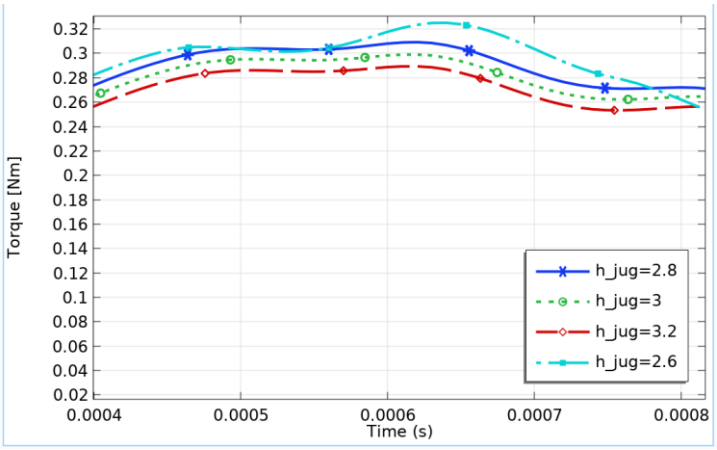


d) Torque-time variation curves for different stator yoke heights *h_jug*.

Fig. 2. Torque-rotor positions for different geometrical constructive parameters (computed for 1/6$^{th}$ of a period, T/6 = 0.4 ms).

The electromagnetic torque was determined with *Arrkio's relation*, which is a variant of the *Maxwellian tensor* method that consists, for 2D models, in a surface integral between the two radii placed at the level of machine's airgap multiplied with motor ideal axial length $l_i$:

$$T = \frac{l_i}{\mu_0 (r_e - r_i)} \int_S r B_r B_\varphi dS \tag{2}$$

where $S$ is the airgap area comprised between an internal radius $r_i$ and external radius $r_e$, $B_r$ and $B_\varphi$ are the radial and tangential magnetic flux densities. Due to integration on a curve rather than a surface $S$, the *Maxwellian tensor*, which is the implicit method used in COMSOL for torque computation, is less accurate than *Arrkio's method* [7,10,12].

In fig. 2 are shown various torque-time curves reflecting various optimization stages done to achieve a torque with less possible ripple. Among the modified geometrical parameters were: *h_jug* – the stator yoke height; *r_umar* – the radius of the rotor within two consecutive permanent magnets; *l_istm* – the slot opening; *alpha* – the permanent magnet pole pitch [13]. The final torque-rotor position variation is shown in fig. 3. Despite the optimization, the torque ripple remains noticeable, but that is specific to BLDC motors with switched commutation. In contrast, the continuous rotation of the stator magnetic field in AC brushless motors generates a smoother operation, with less torque ripple [3,14] .

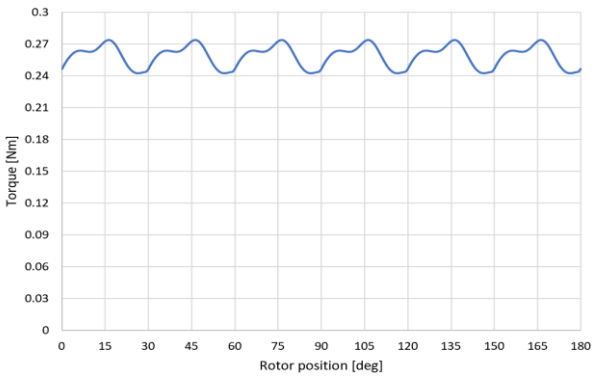


Fig. 3. The torque has some ripple, which is specific to concentrate windings.

### 3. Eddy currents computation

Eddy currents in the stator sleeve were computed from FEM numerical solution in two different ways. The first method consisted in computing directly Joule losses in the stator liner:

$$P_F = l_i \int_S \rho \cdot J_F^2 dS \tag{3}$$

with $l_i$, the ideal axial length of the motor, $\rho$ the material resistivity (the material used was Hastelloy C-4 with electric resistivity 1.25x10-6 Ωm), $J_F$ Foucault current density and $S$ the stator can area (where eddy currents are induced, fig. 4).

The second method consists in computing the torque with and without eddy current losses in the stator liner. The difference between torque values (top

line and bottom lines in fig. 5) is noted with $M_F$ and represents the breaking torque caused by eddy currents.

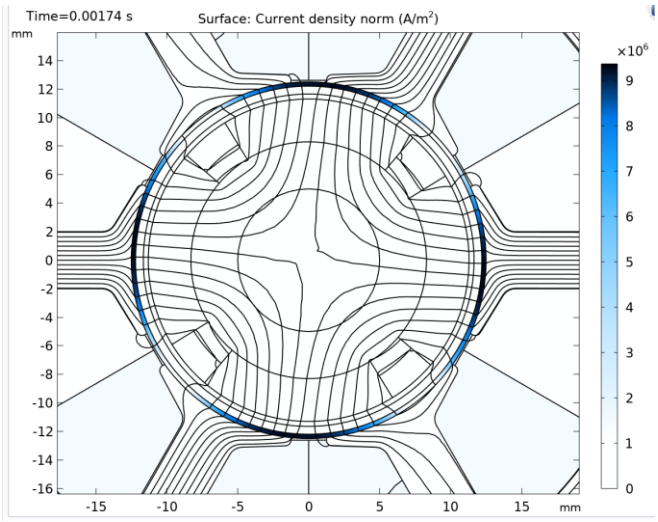


Fig. 4. Eddy currents in the stator sleeve in A/mm$^2$ at time t = 0.00174s).

The two torque-time variations (solid blue and dot green curves in fig. 6) are computed for two stator liner widths, higher torque corresponding to the narrower liner. The eddy current losses are given by $P_F = M_F$ x $\Omega$, with $\Omega$ the angular speed. Both methods used produced a similar result, with $P_F$ = 86W when computed directly with eq. (3), or 84.2 W when computed from torque difference for the stator with 0.35mm can.

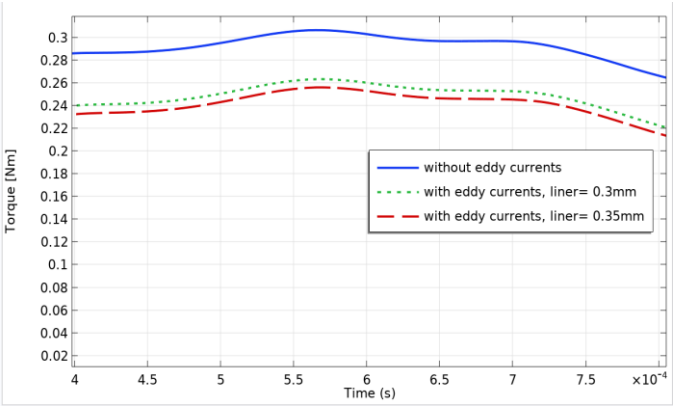


Fig. 5. Torque computed at same current and stator liner width:
a) 0.35mm, b) 0.30 mm and c) no eddy currents considered in the liner.

The eddy currents produce the largest losses inside the motor making its cooling more challenging. The reduction of eddy current losses to 74 W, fig. 6., or 71.9W computed using torque difference, can be achieved by diminishing the stator inner sleeve thickness from 0.35mm to 0.30mm.

As expected, Foucault losses are proportional to the stator liner width as the magnetic field is perpendicular to it (compared to eddy current losses in the laminations of an electrical machine, proportional to the square of the lamination width, as magnetic field direction is along the laminations) [8].

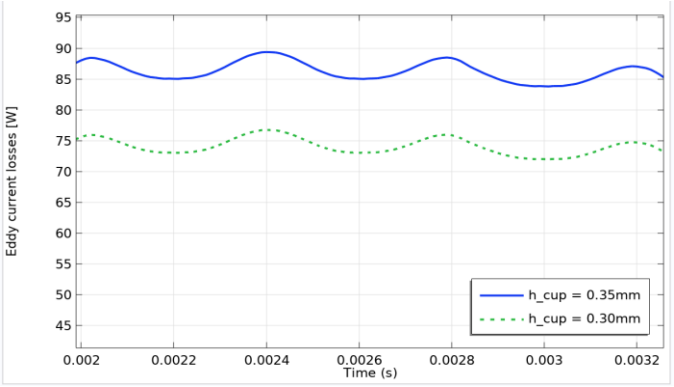


Fig. 6. Eddy currents losses variation as rotor moves, for stator liner thickness: a) 0.35mm, b) 0.3mm.

As eddy current losses are very important to motor final design and its cooling, and because the 2D model considers currents having only axial direction, a 3D model was developed, fig 7.

The eddy current losses obtained from the 3D model, fig. 8 are 69W smaller than 84W computed with the 2D model. In fig. 9 the power losses time variation is plotted. Despite some numerical incertitude, the pre-design calculations are given a good feeling of the magnitude of the eddy current losses and the design measures that should be considered for their limitation. Among those, is reducing the stator liner thickness to a minimum technologic value and usage of Hastelloy C-4, a metallic alloy with very low electrical conductivity. Using carbon fiber or a rigid plastic as the material for the stator liner to annul eddy currents completely was not considered for this model, as that would imply increasing liner thickness and the motor total airgap, generating a torque decrease.

To compute the motor back EMF, the field model was coupled with the circuit equation. In eq. (1) current density was not given, but it resulted from the stator circuit equation $V = R_L I_{coil}$. As the generated current is negligible due to the very high value of the load resistance $R_L$, the machine's terminal voltage $V$ equals back EMF. To compute the maximum EMF the rotor is spined at no-load speed, and it should not exceed supplied voltage [9,11,12].

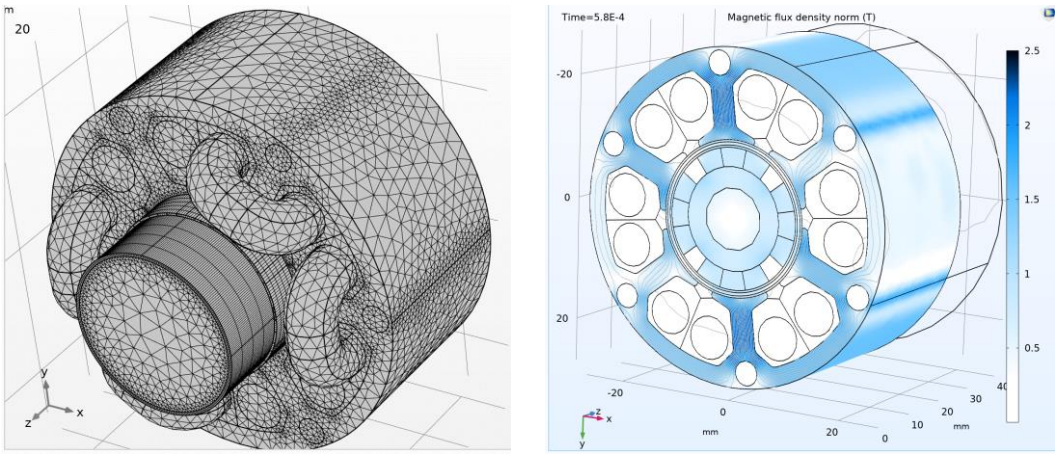


a) b)

Fig. 7. The motor 3D model used for computing eddy currents in the stator liner: a) discretization mesh, b) magnetic flux density and field lines.

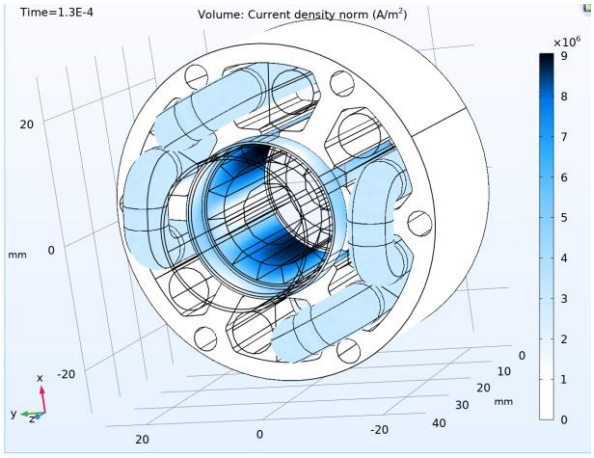


Fig. 8. The current density distribution in the motor [A/m2] (light blue - the current density in the two active phases; eddy currents do not have a constant value in axial direction and have higher values in front of the permanent magnets).

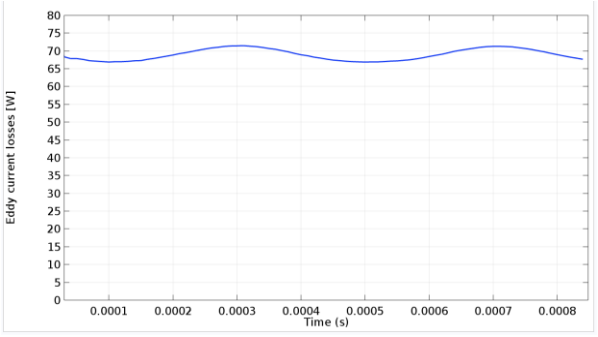


Fig. 9. Eddy current losses time variation was obtained from 3D calculation at 12,500 rpm.

As shown in fig. 10, the line-to-line voltage waveform is not quite trapezoidal, as it should be in BLDC motors, and that is generating some torque ripple. That is also caused by the fact the motor is equipped with a concentrated (tooth) winding to reduce the length of the end turns. Such a winding produces a more sinusoidal back EMF (windings with an integer number of slots per pole and phase are producing more trapezoidal-shaped EMF, thus more suitable in BLDC machines) [15,16,17].

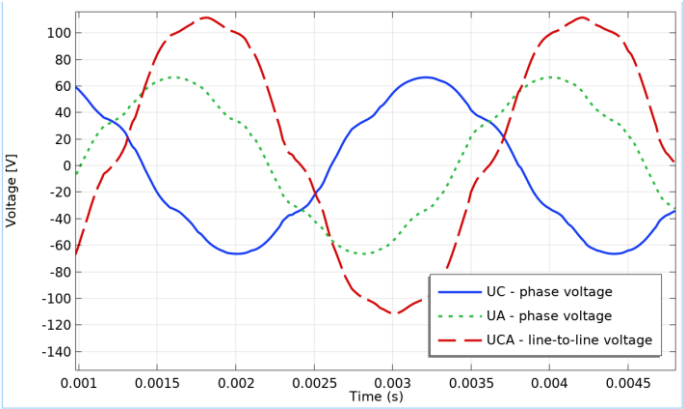


Fig. 10. Motor line-to-line and phase back EMF. For 30 turns per coil, the line voltage value falls under the maximum available voltage of 120V.

## 4. Conclusions

Designing, optimizing, and analyzing BLDC motor performance using numerical modeling represent a modern and powerful tool. Combining field FEM model with simple but needed circuit equations allowed precise dimensioning of the coil number of turns, by computing motor back EMF. The parametrized geometry of the motor, modeled using COMSOL Multiphysics, allowed its optimization resulting in a torque-time variation with minimal ripple.

While in high-speed BLDC motors, the rotor permanent magnets must be capped to resist centrifugal forces, there are also cases when the stator should be protected by a liner to prevent, for example, a fluid penetration to the motor coils. In such situations, the eddy current generated by permanent magnets in the stator cup is important and can generate most of the losses in the motor. The model proposed here showed that losses can be computed in a couple of ways and, while a 3D model will be more precise, a 2D model will also suffice. Compared with other professional software, COMSOL Multiphysics allows modeling 3D coils with their exact spatial distribution of the current density, making more precise the computation. Regardless of using 2D or 3D models, the numerical analysis

will provide more information than any analytical calculations about the eddy current distribution and losses.

## R E F E R E N C E S

[1] http://haynesintl.com/docs/default-source/pdfs/new-alloy-brochures/high-temperature-alloys/brochures/x-brochure.pdf?sfvrsn=15b829d4_40, 29.07.2021.
[2] *T. J. E. Miller*, "Brushless Permanent-Magnet and Reluctance Motor Drives", Oxford Science Publications 1989.
[3] *J.R. Hendershot, T.J.E. Miller*, "Design of Brushless Permanent-Magnet Machines", Motor Design Books LLC; Second Edition, 2010.
[4] *C. C. Chan, J. Z. Jiang, W. Xia and K. T. Chau*, "Novel wide range speed control of permanent magnet brushless motor drives", IEEE Trans. on Power Electronics, vol.10, Sept. 1995, pp. 539 - 546.
[5] COMSOL Multiphysics, v 5.3, Reference Manual, User's Guide, Copyright© 1998-2018.
[6] *N. Sadowski, Y. Lefevre, M. Lajoie-Mazenc, J. Cros*, "Finite Element Torque Calculation in Electrical Machines while Considering Movement", IEEE Trans. On MAG, vol. 28, No.2, March 1992, p. 1410-1413.
[7] *Arkkio*, "Analysis of Induction Motors Based on the Numerical Solution of the Magnetic Field and Circuit Equations", Ph.D. Thesis, Helsinki 1987, UDC 621.313.33 : 519.62/.64.
[8] *J. Liang, A. Parsapour, Z. Yang, C.s Caicedo-Narvaez, M. Moallem, B. Fahimi*, "Optimization of Air-Gap Profile in Interior Permanent-Magnet Synchronous Motors for Torque Ripple Mitigation", IEEE Transactions on Transportation Electrification, Vol. 5, No. 1, March 2019.
[9] *N. Bianchi, L. Alberti Michele Dai Prè, E. Fornasiere*, Theory and Design of Fractional-Slot PM Machines, CLEUP, 2007.
[10] *O. Craiu, T. I. Ichim, L.M. Melcescu*, "Practical Aspects Regarding COMSOL CAD Models Used for Designing a Brushless DC Motor", APME 2019 – SME ediția XV.
[11] *A. Semon, L. Melcescu, O. Craiu and A. Crăciunescu*, "Design Optimization of the Rotor of a V-type Interior Permanent Magnet Synchronous Motor using Response Surface Methodology," *2019 11th International Symposium on Advanced Topics in Electrical Engineering (ATEE)*, 2019, pp. 1-4, doi: 10.1109/ATEE.2019.8724856.
[12] *O. Craiu, T.I. Ichim*, "FEM – PWM Circuit Model of a Brushless DC Motor Using COMSOL", International Symposium on Fundamentals of Electrical Engineering, Bucharest, 5-7 November 2020.
[13] *P. P. Ling, Dahaman Ishak, T. L. Tiang*, Influence of magnet pole arc variation on the performance of external rotor permanent magnet synchronous machine based on finite element analysis, 2016 IEEE International Conference on Power and Energy (PECon).
[14] *D. Hanselman*, Brushless Permanent Magnet Motor Design, 2nd ed.: Magna Physics Publishing, ISBN: 1-881855-15-5.
[15] *N. Bianchi, S. Bolognani, M.D. Pre, G. Grezzani*, Design considerations for fractional-slot winding configurations of synchronous machines, IEEE Transactions on Industry Applications, Vol. 42, No. 4, p.997-1006, 2006.
[16] *Williams, M.M., Zariphopoulos, G., And Macleod*, D.J., Performance Characteristics of Brushless Motor Slot/Pole Configurations, Incremental motion control systems and devices Symposium, IMCSD 94, San Jose, CA, June 1994, pp. 145-153.
[17] *N. Bianchi, L. Alberti Michele Dai Prè, E. Fornasiere*, Theory and Design of Fractional-Slot PM Machines, CLEUP, 2007, ISBN: 9788861291225.